In T. Yoshikawa and F. Miyazaki, ed., "Experimental Robotics III," Lecture Notes in Control and Information Sciences 200, p. 269-281, Springer, 1994.

Experiments with an Electrically Actuated Planar Hopping Robot

P. Gregorio, M. Ahmadi and M. Buehler

Centre for Intelligent Machines, Department of Mechanical Engineering, McGill University
Montréal, Québec, Canada, H3A 2A7

Abstract

We have built a planar one-legged robot to study the design, actuation, control and analysis of autonomous dynamically stable legged robots. Our $15kg$ robot is powered by two low power $80W$ DC electric motors, yet it operates in a stable and robust fashion and currently achieves a top running speed of $1.2m/s$. Both design and control borrow heavily from Raibert's work whose robots are actuated by powerful hydraulic actuators. Surprisingly, even with our drastically reduced power available for actuation, only the hopping height controller had to be modified to achieve stable running. As a basis for further improvements we introduce a scalar "locomotion time" variable, which maps one locomotion cycle onto a fixed interval, independent of operating conditions. A dynamical model and a computer simulation have been developed which accurately predict the robot's behavior.

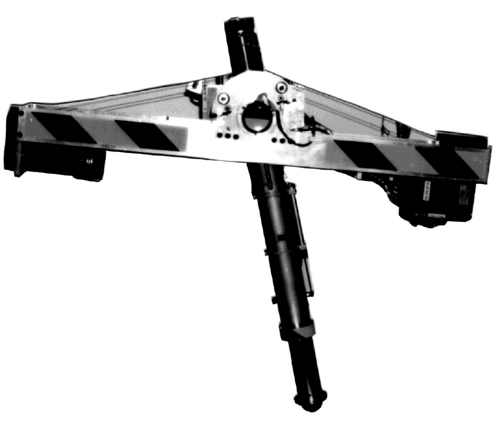

Figure 1: Photograph of the Prismatic Planar Hopping Robot.

1 Introduction

1.1 Motivation

Legged robots which are capable of dynamic operation and balance promise to exhibit similar mobility, efficiency and dexterity as their biological counterparts.

Such robots would be able to operate in a large range of environments and surface conditions and promise to be the mobile platform of choice compared to wheeled systems. However, before legged robots become practical, improved stability properties and autonomous operation are essential. To this end, we focus on electrical actuation, instead of hydraulics, since it is more suitable for indoor autonomous robots, and is a cleaner, safer and a less expensive technology.

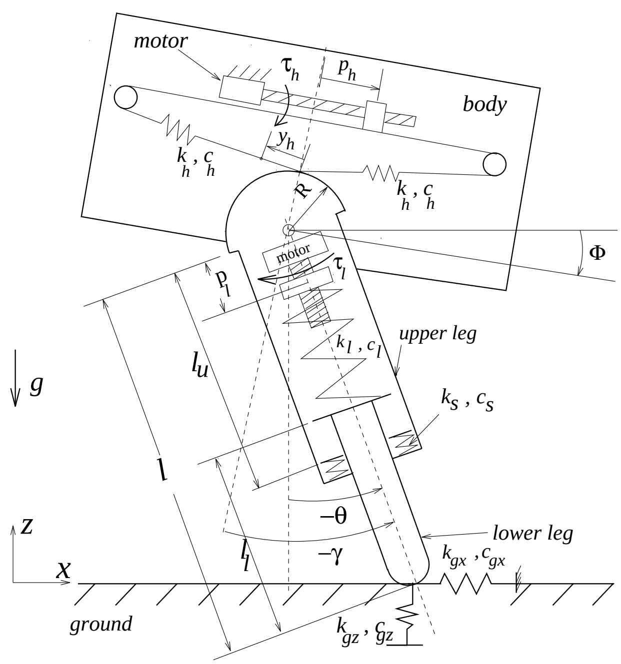

Figure 2: Simplified model of the Planar Hopper

The pioneering work in the field of dynamically stable legged robots has been performed by Raibert [12] whose robots employ powerful hydraulic actuators. His research describes a set of control laws which he was able to apply, with minor modifications, to all of his machines with great success. How much of this control could be applied to machines with much less powerful electric actuators? As our first legged prototype, we designed a planar one legged robot similar to Raibert's planar one-legged hopper, and optimized electric actuation systems for leg and hip.

We found that the the thrust controller for hopping height needed to be modified [10], in order to distribute the power requirements throughout the stance phase. With just this modification, our planar hopper was able to run up to $1.2m/s$. This fact underlines the strength and generality of Raibert's controllers.

In order to apply the same principle of distributing the power requirements throughout the flight phase, we propose to replace the step input command for the leg swing with a continuous path, and implement ground speed matching at touchdown and liftoff, while keeping Raibert's basic foot placement algorithm unchanged. This modification should result in further reduction of power requirements and increase in running speed.

As a next step, we are going to investigate the control of a passive dynamic hip to further decrease the power requirements. This would entail adding a spring in series with the hip actuator such that the unforced response would be close to the running motion. Passive dynamic hip motion has been investigated in the past [14, 6]. Success in harnessing its power for running machines via active control remains elusive. Nature, however, has ample demonstrations of its utility [3, 2, 1].

1.2 Related Work

Experimental research on actively balanced running machines began with Matsuoka [5] who built a planar one-legged hopping machine to study repetitive hopping in humans. His machine was sliding on a 10 degree inclined plane and thrusted by an electric solenoid. The first walking machine with active balance was built by Miura and Shimoyama [7]. It operated with stiff legs, similar to humans on stilts. Our work has been inspired by past research of Marc Raibert [12] who has led the field of dynamically stable legged locomotion during the past decade. He built a variety of running robots, starting with a planar one-legged machine [11], followed by a 3D one-legged, a two-legged planar robot, and a quadruped. His latest robots include a 3D two-legged robot, where each leg has four actuated degrees of freedom. Except for the first one-legged planar hopper, which was pneumatically actuated, his designs are actuated by powerful hydraulic actuators and rely on pneumatics for the leg spring only. This permitted Raibert to focus on robot design and control without being limited significantly by actuator constraints. The strategy was eminently successful and he built many different running robots based on an almost standardized set of custom parts. It is important to realize that all of his robots are controlled by some derivative of the tri-partitioned decoupled control developed for the original one-legged planar hopper [12]. Papantoniou [9, 8] has also built a planar hopper actuated by two electric motors and is using a derivative of Raibert's controller. He employs a clutch which engages the spinning motor at maximum leg compression to maximize energy transfer to the leg. To make this approach work, the stance time needed to be increased considerably to $470ms$, resulting in a mode of operation he terms "compliant walk". There are many more research labs working on dynamic locomotion. An extensive review of research in legged locomotion can be found in [13].

The paper is organized as follows. Section 2 discusses the mechanical design issues relevant to our robot design. Our simulation model is described and verified by comparison to experimental runs in Section 3. Section 4 describes our modifications to Raibert's controller for electric actuation. In Section 5 we present and discuss experimental running data, and discuss further improvements in Section 6.

2 Design

2.1 General Considerations

The planar, one-legged robot currently being studied is an elaboration of our electrically actuated, vertical hopping robot. The robot is comprised of two systems. The prismatic leg serves to excite and maintain a harmonic, vertical oscillation. Mechanical design considerations for the leg are discussed in [10]. In order to allow forward running, the leg attaches to the robot body through an actuated hip. This hip actuation system must allow for the control of the leg angle essential to stable forward running. Since only the relative angle between the body and leg can be actuated, it is desired to have a high ratio of body inertia to leg inertia so that the leg can swing with minimum body pitching. Conversely, low body mass is desirable to reduce overall energy requirements. These requirements dictated a horizontally long body with concentrated masses located at the ends. This morphology is evident in Figure 1.

The hip torque requirements for leg swing during forward running (up to $55Nm$) necessitate a gear ratio of about 30:1 between our 80W motor with $1.78Nm$ stall torque and the hip. Moreover, the design should allow for the insertion of a spring in series with the hip motor. Our design uses a high efficiency ballscrew (similar to the one for leg actuation) coupled to the motor through a miniature HTD belt and unity ratio pulleys. This arrangement allows the motor to be placed underneath the ballscrew and results in a body length below our desired maximum of $1m$. The ball nut is attached to cables which run over idlers and connect to a pulley attached to the leg and centered at the hip as illustrated in Figure 2. This basic configuration was optimized as discussed in the following section. As implemented, this system provides a gear ratio of 30:1 between motor and hip and allows for simple inclusion of compliance in the cables. Even for direct actuation, the Spectra cables provide enough compliance to protect the ballscrews from excessive impulsive forces at touchdown or during failures.

2.2 Detail Design

The geometric model depicted in Figure 2 presents the parameters relevant to the design of the actuated hip and Table 1 contains the basic nomenclature. Although the current robot uses direct actuation for leg angle servoing, compliance may be added in the future and our design optimization takes both direct and compliant actuation cases into account. An identical model is used to analyze both cases, but for direct actuation we assign a large stiffness to the hip springs k_h. Validation of this assumption was confirmed through simulation.

The design problem is to select the design parameters under our control, namely the pulley radius, the ballscrew lead and the spring stiffness. We specify a periodic desired hip angle and require that the driving motor remains within its specified torque-speed limits. To simplify the analysis we assume that the body is stationary. A sinusoidal path is considered for the hip angle θ which is close to the leg motion in the passive running case. Based on the equations of motion of a ball screw,

x	body horizontal position (m)
z	body vertical position (m)
l_c	leg C.G. to hip displacement
m_l	leg total mass (kg)
k_s	stopper model stiffness (N/m)
c_s	stopper model damping $(N/m/s)$
θ_m	hip motor angle angle (rad)
m_{hs}	hip ball nut mass (kg)
J_{hs}	hip ball screw inertia (kgm^2)
F_h	hip spring force (N)
r_h	leg ball screw lead (m/rad)

Table 1: Nomenclature

$$\tau_h = r_h F_h - \alpha_h \ddot{p}_h \tag{1}$$

with

$$\alpha_h = J_{hs}/r_h + r_h m_{hs},$$

the expression for the hip string force

$$F_h = 2k_h(y_h - p_h) + 2c_h(\dot{y}_h - \dot{p}_h) \tag{2}$$

and a small angle approximation $sin(\theta) \approx \theta$ we obtain for the hip dynamics

$$J_l\ddot{\theta} = RF_h - C_t\dot{\theta} - m_l g l_c \theta. \tag{3}$$

Solving (3) for a prescribed sinusoidal path $\theta = \theta_0 \sin(\omega t)$ with $\theta_0 = 0.35$ and $\omega = 4\pi rad/sec$ requires a hip torque

$$\tau_h = A\sin(\omega t) + B\cos(\omega t) \tag{4}$$

where A and B are functions of the system design parameters, primarily the lever arm R, the stiffness k_h and ball screw lead r_h (equivalently L in mm/rev). We can now evaluate the motor's torque–speed requirements for this motion $\tau_h(\omega)$, where the maximum torque depends on the design parameters in a simple fashion,

$$\tau_{max} = \sqrt{A^2 + B^2}.$$

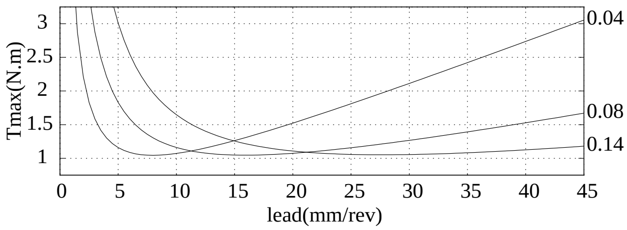

Figure 3: Maximum required torque vs L and different R for direct actuation case

This problem cannot be cast as a straightforward standard numerical minimization problem, since there are many non-standard constraints. For example, the motor characteristics require that the maximum torque be a function of the velocity. Furthermore ball screws are available only in coarsely discrete leads and lengths and their inertial parameters are only available via lookup tables.

The generated hip force F_h should be kept small since it affects the overall size and weight of our structures. Since we plan to use elastomeric springs, the spring stiffness was limited to $5kN/m$ due to energy storage limitations. The ball screw travel should be less than $10cm$ to limit the inertia, mass and body length. The design is further complicated by the necessity to meet the constraints for both direct and compliant actuations. The compliant case is facilitated by large pulley radius R, resulting in smaller torque requirements, but this increasing R, when combined with the optimum lead (Figure 3), increases motor velocity, acceleration, ball screw travel and lead in the direct actuation case.

The final design parameters of lead $L = 16mm$, pulley radius $R = 0.08$ and spring constant $k_h = 3600$ are an attempt to satisfy all the constraints concerning pulley radius, ballscrew lead, maximum motor torque and velocity, as well as the resulting ballscrew travel. This set of parameters minimizes the motor torque-speed requirements for the compliant hopper by matching the natural frequency of the system with the frequency of the vertical oscillations of about $2Hz$ [10].

3 Simulation

In parallel with our experimental work, we developed a planar six degree of freedom (seven d.o.f if the hip is compliant) simulation based on the model depicted in Figure 2. The vertical dynamic model from [10] has been expanded to include the full planar dynamics. In contrast to our analytical model which contains distinct stance and flight models, the simulation employs only the flight model, and implements the ground interaction during stance via an external force applied at the toe generated by the ground spring-damper model. In Figure 4, a comparison of the vertical body height and the leg actuator length obtained from simulation and an experimental run validates our model.

The simulation is set up such that we can develop and verify control code, and subsequently transfer it to the runtime environment with minimal modification. Moreover, the validated model can now be used for analytical performance studies and controller development.

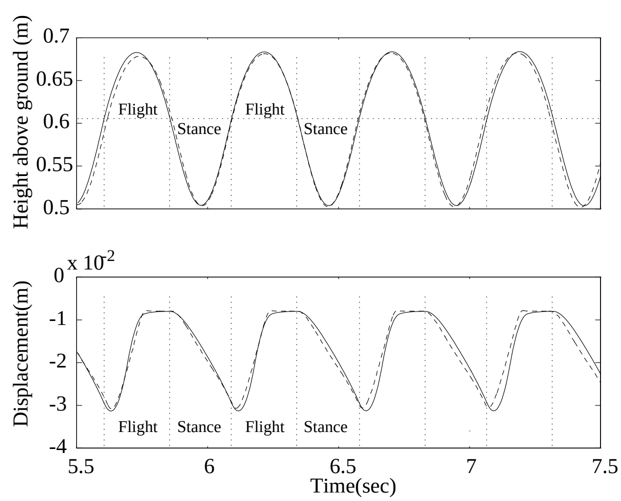

Figure 4: Hopping height and actuator displacement comparisons. Solid Line: Simulation, Dashed line: Experiment

4 Control

We took Raibert's three part control algorithm [12] and applied minimal modifications as described below.

Vertical Motion (Hopping height):
"Apply a constant position step to the leg actuator at

time of maximum compression."

At maximum compression, the ground force acting against the leg actuator is approximately $500N$, which makes this an impractical strategy with low power electric actuators. Instead we use a different open loop controller described in [10],

$$\tau = \bar{\tau}(1 - \frac{\omega}{\hat{\omega}}),$$

which specifies a scaled version of the maximum torque-speed curve of our motor given by

$$\tau \leq \hat{\tau}(1 - \frac{\omega}{\hat{\omega}})$$

with $0 \leq \bar{\tau} < \hat{\tau}$ in the first quadrant (stance), and a high gain PD controller to return the actuator during flight. This strategy is exactly implementable and applies thrust continuously during the stance phase. For our experiments we chose $\bar{\tau} = 1Nm$ with $\hat{\tau} = 1.78Nm$.

Forward speed (Foot placement algorithm, FPA): Raibert's FPA

$$x_f = \frac{\dot{x}T_s}{2} + \kappa_{\dot{x}}(\dot{x} - \dot{x}_d)$$

was adjusted for treadmill running, with $\dot{x}$ replaced by $\dot{x}_{TM} + \dot{x}$. In addition, an "integral" term to servo the robot around the center of the treadmill was added. The FPA implementation is thus given by

$$x_f = \frac{\dot{x}_{TM}T_s}{2} + \kappa_x(x - x_d) + \kappa_{\dot{x}}(\dot{x} - \dot{x}_d) \qquad (5)$$

where x is the robot's position.

Body Attitude (Pitch control):

$$\tau = \kappa_p(\phi - \phi_d) - \kappa\dot{\phi}$$

This controller was left untouched.

5 Experiments

The hopping robot illustrated in Figure 1 was constrained to move in a vertical plane through a virtual motion system (VMS). The VMS is a planarizer consisting of horizontal and vertical ball slides and a revolute joint. All three degrees were instrumented with optical encoders to measure the horizontal and vertical position and the pitch (body angle). An electric $5hp$ treadmill was installed beneath the VMS allowing unlimited horizontal travel for robot running.

5.1 Position Tracking

The simplest form of planar motion is vertical hopping with a horizontal disturbance. In Figure 5 we see the response of the hopping robot to step inputs in desired horizontal position. Control of horizontal position is achieved through the modified FPA discussed above. Stable position control is evident for horizontal perturbations on the order of one third the leg length.

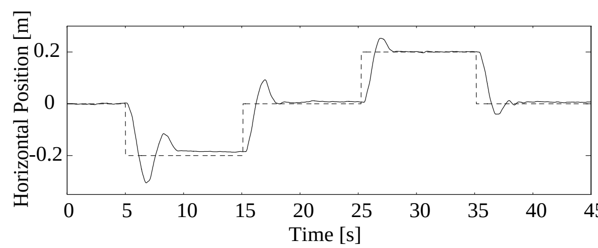

Figure 5: Horizontal position regulation. *The dashed line is the horizontal setpoint while the solid line indicates the robot position.*

5.2 Velocity Tracking

Beyond position regulation, velocity tracking is the essence of planar running. Since our robot runs on a treadmill, any steady state speed error would result in an increasing position error and the robot would quickly exceed the limits of treadmill size. Our modified version of the FPA (5) introduces an integral term to eliminate the velocity steady state error and thus limit the position error with respect to the treadmill center. Therefore the treadmill speed in Figure 6 is roughly equivalent to the robot running speed.

Figure 6 shows small scale variations in the treadmill speed due to toe impact at touchdown (upper solid curve) and the limited bandwidth of the treadmill velocity controller. Deviations from the desired position at treadmill centre are limited to 0.2m (lower dashed curve) while the robot speed varied between 0 and $1.05m/s$. The total distance traversed was $26m$.

5.3 Pitch Control

As the robot leg swings throughout locomotion, the body also pitches freely. Due to its large mass and inertia, any instability in the body pitching motion can quickly destabilize the entire running cycle. Thus

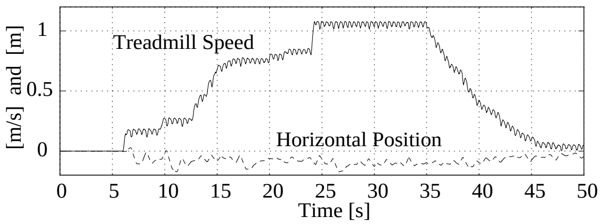

Figure 6: Velocity tracking for forward running. *The treadmill speed is manually regulated from zero, vertical hopping, to* $1.05 m/s$ *and back to zero (upper, solid curve). The lower dashed curve shows the robot deviation from the centre of the treadmill.*

control of body pitching during stance is critical to stable running.

Figure 7 shows the cyclic oscillations of the robot body (lower solid curve) as the forward speed increases to $0.97 m/s$. Despite the large variation in speed the robot's pitching oscillation is kept within only $2 deg$ of the horizontal.

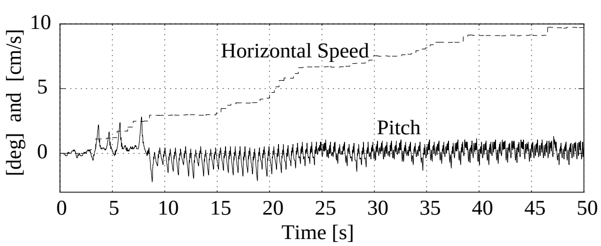

Figure 7: Body pitching during forward running. *The cyclic pitching motion of the robot body about the hip is kept to an amplitude of* $2 deg$ *(solid, lower curve) while the robot accelerates on the treadmill to* $0.97 m/s$ *(upper dashed curve).*

6 Improvements

From the previous sections, it is apparent that Raibert's control, with minor modifications, results in very good performance even on our electrically actuated robot. This attests to the fundamental nature of the algorithm, and, to some extent, to the sound design principles employed in our robot. In this section, we are describing our ongoing efforts toward further improving the robot's efficiency necessary for autonomous operation.

6.1 Locomotion Time

A scalar variable indicating the fraction of flight or stance time that has been elapsed, would be of general utility for control. It will be used, for example, in our online trajectory calculations for ground speed matching and power minimization. Such a measure is

$$\epsilon \triangleq \frac{\dot{z}}{\sqrt{2g(z - z^*) + \dot{z}^2}}. \tag{6}$$

This is the same measure as the "phase angle" introduced in [4] which was critical for the stable coordinated control of the "two-juggle," a robotic juggling task with two pucks. For vertical hopping, with touchdown and liftoff position at z^* the locomotion time (6) maps a flight (or stance) phase onto the interval $(-1, 1)$ between liftoff and touchdown, with $\epsilon = 0$ at apex (max. compression). Moreover, if we assume zero dissipation during flight phase, its derivative is constant. Figure 8 shows the locomotion time computed online for an experimental run.

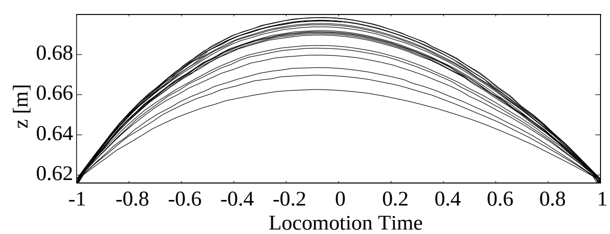

Figure 8: Locomotion Time vs. z for vertical hopping.

6.2 Speed Matching

At present, after liftoff, a high gain PD controller servos the leg toward its desired touchdown angle, as calculated from the foot placement algorithm (5). Since convergence must be assured for even short flight times, high gains are necessary, resulting in unnecessarily jerky motion for longer flight times and large transient hip torques. Furthermore, the leg is servoed to zero touchdown angular velocity, and upon ground contact is forcefully accelerated backwards. Both of these drawbacks can be alleviated using a reference leg trajectory during flight based on locomotion time. At liftoff and at touchdown, a parabola is matched to actual (liftoff) and desired (touchdown) leg trajectory.

The parabolas are joined by a straight line tangent to both. Figure 9 compares the proposed reference trajectory to the actual flight phase path for forward running at $0.7m/s$.

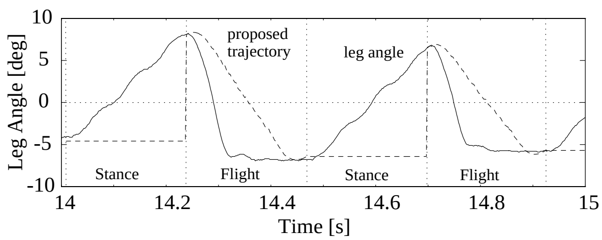

Figure 9: Actual leg swing and proposed reference trajectory. *The solid curve shows the cyclic swinging motion of the robot leg about the vertical position, zero leg angle, for running at 0.7 m/s. During the flight phase the leg angle is servoed to a desired touchdown value that will assure stable running. The broken line indicates the proposed reference trajectory. This trajectory terminates at the same touchdown setpoint but additionally matches the leg swing rates at liftoff and touchdown.*

6.3 Passive Dynamics

During flight, the hip motor has to decelerate sharply, accelerate and then decelerate the leg, which requires peak power of our motors at $1m/s$. Most of this return swing motion of the leg can be provided by a properly dimensioned spring in series with the hip actuator. This has been proposed and experimentally tested in passive (unstable) mode by Raibert [14]. Our robot has been designed to accommodate such springs. We are currently implementing them and will report on this research in the near future.

7 Conclusions

We have presented the design of an electrically actuated planar one-legged hopping robot, as a research vehicle for autonomous legged systems. Raibert's controller was modified to reduce the power requirements for the leg actuation and was shown experimentally to achieve stable running up to 1.2 m/s. To reduce power requirements further, we proposed a locomotion time based flight trajectory which also implements ground speed matching. Finally, we are currently pursuing the application of controlled passive dynamic hip motion.

We are also in the process of replacing the prismatic leg joint with an articulated leg. This will, in addition to a reduction in friction, also improve the robot's dexterity, and greatly improve its reliability. Finally, the friction properties of revolute joints are much more constant over time, which will simplify the application of analytical results based on theoretical models. In the future we will also emphasize the derivation of analytical results to eliminate or at least minimize the need for empirical gain settings, which requires excessive amounts of time, even for our current relatively simple machine.

References

[1] R. McN. Alexander. Three Uses for Springs in Legged Locomotion. *Int. J. Robotics Research*, 9(2), 1990.

[2] R. McN. Alexander, N. J. Dimery, and R. F. Ker. Elastic Structures in the back and their role in galloping in some mammals. *J. Zoology (London)*, 207, 1985.

[3] R. McN. Alexander and A. Vernon. The mechanics of hopping by kangaroos. *J. Zoology (London)*, 177, 1975.

[4] M. Buehler, D. E. Koditschek, and P. J. Kindlmann. Planning and Control of Robotic Juggling and Catching Tasks. *Int. J. Robotics Research*, (accepted: 17. Dec. 91).

[5] K. Matsuoka. A mechanical model of repetitive hopping movements. *Biomechanisms*, 5:251–258, 1980.

[6] T. McGeer. Passive dynamic walking. *Int. J. Robotics Research*, 9(2), 1990.

[7] H. Miura and I. Shimoyama. Dynamic walk of a biped. *Int. J. Robotics Research*, 3:60–74, 1984.

[8] K. V. Papantoniou. Control architecture for an electrical, actively balanced multi-leg robot, based on experiments with a planar one leg machine. In *Proc. Int. Fed. Automatic Control*, pages 283–290, Vienna, Austria, 1991.

[9] K. V. Papantoniou. Electromechanical design of an actively balanced one leg electrically powered robot. In *Proc. IEEE Conf. Intelligent Systems and Robots*, Osaka, Japan, 1991.

[10] H. Rad, P. Gregorio, and M. Buehler. Design, modeling and control of a hopping robot. In *Proc. IEEE/RSJ Conf. Intelligent Systems and Robots*, Yokohama, Japan, Jul 1993.

[11] M. H. Raibert. Dynamic stability and resonance in a one-legged hopping machine. *4th Symp. Theory and Practice of Robots and Manipulators*, 1981.

[12] M. H. Raibert. *Legged Robots That Balance*. MIT Press, Cambridge, MA, 1986.

[13] M. H. Raibert. Legged robots. In P. H. Winston and S. A. Shellard, editors, *Artificial Intelligence at MIT*, pages 149–179. MIT Press, Cambridge, MA, 1990.

[14] M. H. Raibert and C. M. Thompson. Passive dynamic running. In V. Hayward and O. Khatib, editors, *Experimental Robotics I*, pages 74–83. Springer-Verlag, NY, 1989.